Sulfuric acid in the Amazon Basin: Measurements and evaluation of existing sulfuric acid proxies

Deanna C. Myers[1], Saewung Kim[2], Steven Sjostedt[3], Alex B. Guenther[2], Roger Seco[4], Oscar Vega Bustillos[5], Julio Tota[6], Rodrigo A. F. Souza[7], and James N. Smith[1]

[1]Department of Chemistry, University of California, Irvine, USA
[2]Department of Earth System Science, University of California, Irvine
[3]Morgan Community College, Fort Morgan, CO, USA
[4]Institute of Environmental Assessment and Water Research (IDAEA-CSIC), Barcelona, Catalonia, Spain
[5]Instituto de Pesquisas Energéticas e Nucleares, Cidade Universitaria, São Paulo, Brazil
[6]Universidade Federal do Oeste do Pará, Santarém, Brazil
[7]Escola Superior de Tecnologia, Universidade do Estado do Amazonas, Manaus, Brazil

Correspondence: James N. Smith (jimsmith@uci.edu)

Abstract. Sulfuric acid is a key contributor to new particle formation, though measurements of its gaseous concentrations are difficult to make. Several parameterizations to estimate sulfuric acid exist, all of which were constructed using measurements from the Northern Hemisphere. In this work, we report the first measurements of sulfuric acid from the Amazon Basin. These measurements are consistent with concentrations measured in Hyytiälä, Finland, though unlike Hyytiälä there is no clear correlation of sulfuric acid with global radiation. There was a minimal difference in sulfuric acid observed between the wet and dry seasons in the Amazon Basin. We also test the efficacy of existing proxies to estimate sulfuric acid in this region. Our results suggest that nighttime sulfuric acid production is due to both a stabilized Criegee intermediate pathway, and oxidation of SO_2 by OH, the latter of which is not currently accounted for in existing proxies. These results also illustrate the drawbacks of the common substitution of radiation for OH concentrations. None of the tested proxies effectively estimate sulfuric acid measurements at night. For estimates at all times of day, a recently published proxy based on data from the boreal forest should be used. If only daytime estimates are needed, several recent proxies that do not include the Criegee pathway are sufficient. More investigation of nighttime sulfuric acid production pathways is necessary to close the gap between measurements and estimates with existing proxies.

1 Introduction

Numerous studies have shown that sulfuric acid (H_2SO_4) contributes significantly to atmospheric particle concentrations. It has been found to be a key component in the formation of new atmospheric aerosol particles (Almeida et al., 2013; Jen et al., 2016; Fiedler et al., 2005; Korhonen et al., 1999; Kuang et al., 2010; Kulmala et al., 2012, 2004; McMurry et al., 2000; Myllys et al., 2019; Weber et al., 1996, 1997; Yao et al., 2018), and a significant contributor to the growth of new particles (Bzdek et al., 2012; Paasonen et al., 2010; Riipinen et al., 2007; Stolzenburg et al., 2005, 2020; Wehner et al., 2005). New particle formation (NPF) is a major contributor to global cloud condensation nuclei populations (Gordon et al., 2017; Kerminen et al.,

2012; Spracklen et al., 2008, 2010). Given its importance in atmospheric particle formation and growth, accurate measurements of atmospheric H_2SO_4 concentrations are necessary for understanding atmospheric chemical and thermal processes and accurately simulating new particle formation (Dunne et al., 2016). However, this has been difficult to achieve because of low ambient concentrations ($10^6 - 10^7$ molecules cm^{-3} or lower), which can only be measured using specialized instrumentation such as chemical ionization mass spectrometers (CIMS) (Dada et al., 2020; Eisele and Bradshaw, 1993; Jokinen et al., 2012; Mikkonen et al., 2011), and because of challenges in deploying and operating these instruments.

Due to these challenges, several studies have developed parameterizations to serve as proxies for H_2SO_4 concentrations using its atmospheric sources and sinks (Lu et al., 2019; Weber et al., 1997; Mikkonen et al., 2011; Petäjä et al., 2009). Using measurements of hydroxyl radical (OH) and sulfur dioxide (SO_2), Weber et al. (1997) estimated the daytime concentration of H_2SO_4 with known rates of photochemical production and loss by condensation onto existing particle surface area (condensation sink, CS) and showed good agreement with measurements of H_2SO_4 concentrations made in Hawaii and Colorado, USA. However, like H_2SO_4, OH is difficult to measure due to low concentrations and relatively short atmospheric lifetime (Eisele and Bradshaw, 1993). Since OH is formed via ozone (O_3) photolysis by ultraviolet radiation and OH concentration has been found to correlate well with UV radiation (Rohrer and Berresheim, 2006), radiation has replaced OH concentrations in current H_2SO_4 proxies. This correlation was confirmed by Petäjä et al. (2009), who estimated concentrations of H_2SO_4 in Hyytiälä, Finland using proxies with OH measurements, and UV and global radiation as proxies for OH concentration, and found good agreement between estimated and measured H_2SO_4 concentrations using both UV and global radiation as OH substitutes. Because global radiation is more frequently measured than UV radiation, Mikkonen et al. (2011) used global radiation to develop proxies based on CIMS measurements of H_2SO_4 made in varying environments throughout North America and Europe. They found that the best approximation for all locations depended mainly on radiation strength, with reduced source dependence on the concentration of SO_2, and minimal loss contribution from CS. Mikkonen et al. (2011) attributed the reduced dependence on SO_2 and CS to these species representing particulate pollution, which would act as both H_2SO_4 and OH sinks. Similarly, a proxy developed using measurements of SO_2 concentration, UV radiation, and CS from Beijing, China found that CS plays a relatively minor role in determining concentrations of H_2SO_4 except when CS is large (Lu et al., 2019). A high correlation between CS and SO_2 concentrations was observed, which Lu et al. (2019), like Mikkonen et al. (2011), attributed to both parameters representing atmospheric pollution. Together, the Mikkonen et al. (2011) and Lu et al. (2019) results demonstrate that using only photochemical production and CS as the source and sink, respectively, of H_2SO4 is insufficient to accurately estimate its concentration across a wide range of locations.

More recent work has considered additional sources and sinks for atmospheric H_2SO_4 to improve these estimates. In addition to formation by OH oxidation of SO_2, several proxies described in Dada et al. (2020) consider the formation of H_2SO_4 from O_3 oxidation of biogenic alkenes via stabilized Criegee intermediates (sCI) (Mauldin et al., 2012). This production pathway is hypothesized to dominate at nighttime, when OH is a less important oxidant (Mauldin et al., 1998). The loss term in these new Dada et al. (2020) proxies include both condensation sink and the clustering of H_2SO_4 monomers to form new atmospheric particles. Through testing for a variety of environments, Dada et al. (2020) developed H_2SO_4 parameterizations representing sites with conditions similar to those used to develop and verify these proxies. They suggest comparison of any site's H_2SO_4,

OH, SO_2, O_3, and dominant alkene concentrations, as well as global radiation and CS, to those of the sites studied and use the proxy developed for the environment most similar to that of interest. The Dada et al. (2020) proxies showed good agreement between the measured and estimated concentrations of H_2SO_4 for data from sites used in the proxy construction, but thus far the proxies have been tested on one new environment. Further validation of these proxies is needed by testing them on measurements from a variety of sites.

Though several of the proxies described earlier considered measurements made in varying environments to develop a robust, generalized H_2SO_4 proxy (Dada et al., 2020; Mikkonen et al., 2011), only measurements made in the Northern Hemisphere have been used in their construction. Measurements from the Southern Hemisphere need to be considered in order to develop a proxy that accurately estimates H_2SO_4 concentrations globally. The Amazon Basin has been the focus of recent field work, specifically the Observations and Modeling of the Green Ocean Amazon (GoAmazon2014/5) experiment (Martin et al., 2016), in large part because the biological emissions from the forest contribute significantly to climate and atmospheric composition in South America (Artaxo et al., 2013; Pöschl et al., 2010). This region is characterized by a mixture of pristine biogenic conditions with pollution from Manaus and human activity in the area (Nobre et al., 2016). Natural emissions dominate the wet season (December – May), during which time wet deposition of accumulation mode particles (diameter between $0.1 – 2.5$ μm) and coarse mode particles (diameter greater than 2.5 μm) reduces concentrations of particles in these size ranges compared to the dry season (August - November). However, recent work has shown that anthropogenic pollutants influence atmospheric particles during the wet season as well (Glicker et al., 2019). Previous measurements in the Amazon Basin have reported concentrations of SO_2 that were more than an order of magnitude smaller than those measured in remote sites in the Northern Hemisphere (Andreae and Andreae, 1988; Andreae et al., 1990; Martin et al., 2010). From these measurements, model results have suggested that H_2SO_4 levels are too low to result in surface-level particle formation (Spracklen et al., 2006). However, measurements of H_2SO_4 levels in the Amazon Basin have not yet been reported.

This manuscript reports the first measurements of H_2SO_4 in the Amazon Basin performed using chemical ionization mass spectrometry. The focus of this work is during two intensive operating periods (IOPs) during the GoAmazon2014/5 campaign; one during the wet season (IOP 1: 9 February 2014 – 8 March 2014) and one during the dry season (IOP 2: 28 August 2014 – 5 September 2014). We then assess the efficacy of existing proxy parameterization in estimating H_2SO_4 concentrations in the Amazon Basin, the first location in the Southern Hemisphere to be tested.

2 Methods

2.1 Site description

All chemical and meteorological measurements were performed during the GoAmazon2014/5 campaign at the T3 site (3.2133° S, 60.5987° W), 10 km northeast of Manacapuru, Brazil (Martin et al., 2016). This site is located in pastureland 70 km west of Manaus, Brazil, in central Amazonia. Measurement facilities deployed to T3 included the Atmospheric Radiation Measurement (ARM) Mobile Facility number 1 (AMF-1), the ARM Mobile Aerosol Observing System (MAOS), and laboratories contained in four modified shipping containers with instruments operated by several research organizations. Air masses arriving at this

site typically originate near the coast of the Atlantic Ocean and contain biogenic species from the forest as they travel to the
90 site, with some influence from Manaus. All times are reported in UTC.

2.2 Instrumentation

2.2.1 Trace Gas Analysis

Gas-phase concentration measurements of H_2SO_4 and OH were made using a selected ion chemical ionization mass spectrometer (SICIMS), the details of which have been reported previously in Jeong et al. (2022), Tanner et al. (1997), and Mauldin
95 et al. (1998). Concentrations of SO_2 were measured using a Thermo Fisher Scientific Model 43i trace level-enhanced pulsed fluorescence SO_2 analyzer with a detection limit of 7.4×10^9 molec cm^{-3}. More specific information regarding the operation and calibration of the SO_2 analyzer can be found in Springston (2016). A Thermo Fisher Scientific Ozone Analyzer Model 49i was used to measure concentrations of O_3 based on their absorption of ultraviolet (254 nm) light. More details regarding the operation of this instrument can be found in Springston (2020). Measurements of monoterpene (MT) and isoprene
100 concentrations were obtained using a selected reagent ion proton transfer reaction time-of-flight mass spectrometer (SRI-PTR-TOFMS). These data were calibrated using the ion signal of $C_{10}H_{17}^+$ for α-pinene and $C_5H_9^+$ for isoprene, and α-pinene and isoprene standards. More specific details about the operation of this instrument are reported in Sarkar et al. (2020). All trace gas concentrations are reported as five-minute averages with units of molecules cm^{-3}.

2.2.2 Particle Number-Size Distribution

105 Particle number-size distributions for particles with electrical mobility diameters 10 – 496 nm from 0:00 UTC 5 February – 18:46 16 February, and 11 – 460 nm for the rest of IOP 1 and IOP 2 were collected using a TSI Model 3963 scanning mobility particle sizer with a TSI Model 3772 condensation particle counter (CPC) (ARM, 2014c). Sampled particles were dried to a maximum of 20 % RH before classification (Kuang, 2016). CS was estimated from the number size distributions for particles with mobility diameters 11 – 460 nm using the method described in Kulmala et al. (2001) and Kulmala et al. (2012).

2.2.3 Meteorology

110

Global radiation was measured at the AMF-1 using a precision spectral pyranometer (Eppley) (ARM, 2014b). Data were collected in 60-second intervals. Ambient temperature, relative humidity, wind direction, and wind speed were measured at AMF-1 in 60-second intervals (ARM, 2014a). All meteorological data are reported as 5-minute averages. HYSPLIT air mass back-trajectories were calculated every 6 hours for each day of the measurement period evaluate influence at the site from the
115 upwind city of Manaus (Rolph et al., 2017; Stein et al., 2015).

2.3 Proxies Tested

We used measurements of SO_2 and OH along with estimates of CS to evaluate the efficacy of the simplest H_2SO_4 proxy developed, which includes the photochemical production of H_2SO_4 and loss to particle surface area in estimating the concentration

of H_2SO_4 using the following equation:

$$\frac{d[H_2SO_4]}{dt} = k[OH][SO_2] - [H_2SO_4]CS^{-1} \tag{1}$$

in which k is the temperature-dependent rate constant (DeMore et al., 1997; Sander et al., 2003). Assuming that H_2SO_4 production and loss are in steady-state, Eq. (1) can be rearranged to directly calculate the concentration of H_2SO_4 (Proxy 1, Table 1). To evaluate whether global radiation (GlobRad) is an effective replacement for OH concentrations in the Amazon Basin, we used Proxy 2, where k' replaces the temperature-dependent rate constant k, and is the fitting parameter between the proxy terms and measured concentration of H_2SO_4, similar to the proxy reported by Petäjä et al. (2009) (Table 1). We also used several of the proxies developed from data sets collected at a variety of locations to assess how well they estimate H_2SO_4 concentrations in the Amazon Basin. This includes the proxy Mikkonen et al. (2011) reported that best predicted H_2SO_4 concentrations across all of the locations they tested, where k is the temperature-dependent rate constant for the reaction of OH with SO_2 (DeMore et al., 1997) multiplied by 10^{12} (Proxy 3, Table 1). Recent proxies developed by Dada et al. (2020) that additionally consider H_2SO_4 production via the sCI pathway and loss due to clustering were tested to evaluate the relative importance of these pathways in determining H_2SO_4 concentrations in the Amazon Basin. Based on the values of the characteristic predictor variables ($[H_2SO_4]$, $[SO_2]$, CS, Global radiation, $[O_3]$, [Alkene]) detailed in Figure 9 of that work, we tested proxies representing environments similar to the boreal forest (Hyytiälä, Finland) (Proxy 4), and representing environments similar to the rural location (Agia Marina, Cyprus) used to develop this proxy (Proxy 5). Notably, Proxy 4 is the only proxy tested that includes the sCI production pathway, making it possible to assess nighttime H_2SO_4 estimations, one of the limitations of the proxies that only consider photochemical H_2SO_4 production. The equations corresponding to each proxy (numbered 1 - 5) are shown below in Table 1.

Table 1. Proxies used in this study to estimate sulfuric acid concentrations. Parameter terms defined in Section 2.3.

Proxy	Equation
1	$[H_2SO_4] = \dfrac{k[OH][SO_2]}{CS}$
2	$[H_2SO_4] = \dfrac{k' \cdot GlobRad[SO_2]}{CS}$
3	$[H_2SO_4] = 8.21 \times 10^{-3} \cdot k \cdot GlobRad[SO_2]^{0.62} \cdot (CS \cdot RH)^{-0.13}$
4	$[H_2SO_4] = \dfrac{CS}{2 \cdot (4.2 \times 10^{-9})} + \left[\left(\dfrac{CS}{2 \cdot (4.2 \times 10^{-9})}\right)^2 + \dfrac{SO_2}{4.2 \times 10^{-9}}\left(8.6 \times 10^{-9} \cdot GlobRad + 6.1 \times 10^{-29}[O_3][Alkene]\right)\right]^{\frac{1}{2}}$
5	$[H_2SO_4] = \dfrac{CS}{2 \cdot (2.0 \times 10^{-9})} + \left[\left(\dfrac{CS}{2 \cdot (2.0 \times 10^{-9})}\right)^2 + \dfrac{SO_2}{2.0 \times 10^{-9}}\left(9.0 \times 10^{-9} \cdot GlobRad\right)\right]^{\frac{1}{2}}$

3   Results and Discussion

Table 2 lists the key variables for the proxies used in this study across both IOPs. Due to instrument malfunctions as well as challenges associated with operating this instrument in this remote location, only a select number of days from each IOP

Table 2. Summary of the mean, median, 5 - 95 percentiles, and standard deviation (Sd) of the relevant trace gases, condensation sink, global radiation, and relative humidity measured in the Amazon Basin during this study.

		IOP 1 (wet season)	IOP 2 (dry season)	Campaign (combined)
$[H_2SO_4]$ 10^5	Mean	9.53	3.85	7.89
	Median	7.82	2.59	6.73
molec cm^{-3}	5 − 95 percentiles	5.17 − 20.4	1.05 − 10.8	1.66 − 18.7
	Sd	5.01	3.19	5.21
$[OH]$ 10^5	Mean	11.1	3.85	7.78
	Median	9.49	2.64	6.86
molec cm^{-3}	5 − 95 percentiles	5.42 − 21.9	0.41 − 11.0	0.63 − 20.2
	Sd	5.23	3.49	5.79
$[SO_2]$ 10^{10}	Mean	0.51	0.96	0.73
	Median	0.38	0.72	0.56
molec cm^{-3}	5 − 95 percentiles	0.11 − 3.55	0.94 − 6.08	0.22 − 5.02
	Sd	1.16	1.83	1.72
CS 10^{-3}	Mean	5.45	18.7	11.6
	Median	4.81	17.0	7.54
s^{-1}	5 − 95 percentiles	1.21 − 11.8	5.13 − 38.7	1.56 − 31.7
	Sd	4.77	12.1	11.1
Radiation (> 10)	Mean	614	666	636
	Median	512	646	587
W m^{-2}	5 − 95 percentiles	39 − 1460	57 − 1270	43 − 1370
	Sd	465	393	437
$[O_3]$ 10^{11}	Mean	2.22	4.43	3.14
	Median	1.86	3.66	2.21
molec cm^{-3}	5 − 95 percentiles	0.40 − 5.09	0.36 − 11.2	0.38 − 9.25
	Sd	1.74	3.62	2.89
$[Isoprene]$ 10^{10}	Mean	1.82	3.15	1.98
	Median	1.10	1.98	1.62
molec cm^{-3}	5 − 95 percentiles	0.68 − 6.32	0.72 − 10.2	0.70 − 7.18
	Sd	2.16	4.01	2.77
RH (%)	Mean	90.5	82.5	88.5
	Median	95.3	88.6	94.2
	5 − 95 percentiles	66.5 − 99.6	52.9 − 99.5	99.6
	Sd	10.7	16.1	12.8

are included for analysis. The measurements reported here span 14 days across IOP 1 (9 - 19 February and 5 - 8 March 2014) and 9 days across IOP 2 (28 August - 5 September); thus the campaign data is more representative of measurements made during IOP 1 (61% of the total data points). Table 3 compares the median values of key parameters from the entire campaign to those reported from other studies, which serves both to provide context for our measurements and to assess the appropriateness of parameterizations that have been developed for different locales. Measurements of H_2SO_4 during both IOPs show a small degree of seasonality (IOP 1 median: 7.82×10^5 molec cm^{-3}; IOP 2 median: 2.56×10^5 molec cm^{-3}), indicating that differences between the wet (IOP 1) and dry (IOP 2) seasons do not influence H_2SO_4 to a large degree. The campaign median value (6.73×10^5 molec cm^{-3}) is within the range reported for the forested sites of Niwot Ridge and Hyytiälä, which suggests that the forest environment may be similar enough to allow the use of the boreal forest proxy reported in Dada et al. (2020). Measured H_2SO_4 is a factor of 3-4 less than those from rural (Agia Marina) and urban (Helsinki, Atlanta, Budapest,

Table 3. Comparison of the median of the relevant trace gases, condensation sink, global radiation, and relative humidity observed during this campaign to those reported from other studies.

Location	Manacapuru (this study)	Agia Marina[1]	SPC[2]	Niwot Ridge[2]	Hyytiälä*[1]	Budapest[1]	Beijing*[1]	Atlanta[2]	Helsinki[1]
Type	Forest/Rural	Rural	Rural/Urban	Forest	Forest	Urban	Urban	Urban	Urban
$[H_2SO_4]$ 10^5 molec cm^{-3}	6.73	18.1	24.0	14.0	2.3	10.2	18.1	28.5	25.5
$[SO_2]$ 10^{10} molec cm^{-3}	0.56	0.46	0.59	0.44	0.14	5.45	2.42	3.79	0.87
CS 10^{-3} s^{-1}	7.54	3.63	6.33	3.90	3.01	10.92	22.7	15.1	3.13
Radiation (>10) W m^{-2}	587	272.48	376	207	35.4	300.56	53.62	89	270.6
$[O_3]$ 10^{11} molec cm^{-3}	2.21	-	9.30	13.8	8.87	-	9.91	7.58	-
[Alkene] 10^{10} molec cm^{-3}	1.62	-	-	-	0.27	-	12.1	-	-
RH (%)	94.2	-	67	52	-	-	-	67	-

[1]Dada, et al. (2020); [2]Mikkonen et al. (2011)
*These entries are the average of the two campaigns listed in Table S3 of Dada et al. (2020).

Beijing) environments. In summary, the range of these observations suggests that the general proxy from Mikkonen et al. (2011) (Proxy 3) and boreal Dada et al. (2020) proxy (Proxy 5) may provide reasonable estimations.

Measurements of SO_2 and O_3 (Table 2) similarly show minimal differences between the wet and dry seasons. Table 3 compares these observations with those from other relevant studies. Observed SO_2 concentrations are higher than those from forested sites, and the campaign average is similar to observations from a rural site (Agia Marina) and a mixed urban/rural site (San Pietro Capofiume, Italy, referred to in the table and hereafter as SPC). The observed levels of SO_2 are lower than those from urban sites Helsinki, Budapest, Atlanta, and Beijing. Measurements of O_3 concentrations during both IOPs are lower than those reported for all sites used in the Dada et al. (2020) and Mikkonen et al. (2011) studies.

Measurements of CS are consistent with previous observations from other sites with dry season CS (17.0×10^{-3} s^{-1}) similar to more polluted sites and wet season CS (4.81×10^{-3} s^{-1}) similar to forested and rural sites and one urban site (Helsinki). This difference in CS between the two seasons is mainly driven by a the higher concentration of accumulation mode particles present during IOP 2 (e.g., the average concentration of 50 - 100 nm particles is 1530 cm^{-3}) compared to IOP 1 (average: 300 cm^{-3}) (Fig. S1). The lower concentrations of accumulation mode particles during IOP 1 is consistent with the increased wet deposition of particles during the wet season (Andreae et al., 2004; Yamasoe et al., 2000). The CS measurements support the use of the Mikkonen et al. (2011) proxy and the Dada et al. (2020) boreal and rural proxies.

We compared the concentrations of isoprene and monoterpenes to determine the dominant alkene, which was used in the Dada et al. (2020) boreal proxy (Proxy 4), per the recommendation in that study. Isoprene was observed to have a higher

concentration (campaign median: 1.62×10^{10} molec cm^{-3}) than monoterpenes (campaign median: 3.33×10^9 molec cm^{-3}), and was thus used in the Dada et al. (2020) boreal estimation as the alkene concentration. The isoprene concentrations mea-
sured during the campaign were about an order of magnitude greater than measured monoterpene levels from Hyytiälä, and significantly lower than alkene concentrations measured in Beijing (Dada et al., 2020), supporting the use of the Dada et al. (2020) boreal proxy. The levels of these key variables (CS, H_2SO_4, SO_2, O_3, and isoprene) in estimating the concentration of H_2SO_4 in the Amazon Basin show that the generalized Mikkonen et al. (2011) proxy and both the boreal and rural Dada et al. (2020) proxies may be appropriate to use in this location.
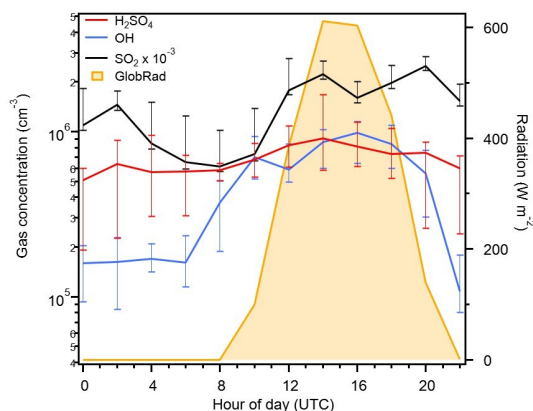
Figure 1. Two-hour diurnal variation of the median H_2SO_4, SO_2, OH, and global radiation measured during the entire campaign. Note that daylight hours are from 08:00 - 22:00 UTC during the campaign; negligible changes between IOPs 1 and 2 were observed.

Next, we compared the two-hour diurnal cycles of the source terms (SO_2, OH, and radiation) in the basic photochemical proxies to assess their correlation with the measured concentrations of H_2SO_4 (Fig. 1). There is no apparent diurnal cycle of H_2SO_4 and, notably, there is not a clear correlation between its concentration and the level of global radiation measured at the site. This is in contrast to the correlation observed between these two parameters at the Northern Hemisphere sites used in the construction of the Mikkonen et al. (2011) and Dada et al. (2020) proxies (data sets from Atlanta, USA; Hyytiälä, Finland; Melpitz, Germany; Niwot Ridge, USA). During the observation period, nighttime concentrations of H_2SO_4 accounted for 36 % of the total measured H_2SO_4, suggesting that while photochemical production is likely an important source of H_2SO_4 Amazon Basin, nighttime sources should also be considered in an efficient proxy.

Additionally, Figure 1 shows that there was OH measured during nighttime (22:00 - 08:00 UTC). This suggests that the common use of global radiation as an OH replacement in H_2SO_4 proxies is only sufficient during daytime hours (08:00 - 22:00 UTC) in the Amazon Basin. This is consistent with model results from Lelieveld et al. (2008, 2016), which indicate that secondary production of OH through O_3 reaction with isoprene is a major source of OH in the boundary layer in the Amazon rainforest, in addition to primary production from photodissociation of O_3. This secondary pathway is active at nighttime, and likely contributes in other regions where data sets have been used to construct and test H_2SO_4 proxies, meaning that nighttime H_2SO_4 is not being accounted for in these estimations. Thus, as we move through our testing of the proxies that substitute

190 global radiation for OH, it is with the understanding that this substitution misses nighttime production of H_2SO_4 through the oxidation of SO_2 by OH, which is likely occurring in this location. We also note that all of the parameterizations tested include only oxidation of SO_2 to produce H_2SO_4, though species such as dimethylsulfide, hydrogen sulfide, and methylmercaptan have been previously measured in the Amazon Basin and may contribute to H_2SO_4 production (Andreae and Andreae, 1988; Andreae et al., 1990).

195 Because the measurement site is located downwind of Manaus, the largest city in the state of Amazonias, we used HYSPLIT back trajectories to differentiate between periods with and without influence from Manaus, both of which occurred frequently during IOPs 1 and 2. The two-hour median diurnal variations of H_2SO_4, SO_2, and OH are shown in Figure S7 of the Supporting Information. During periods with Manaus influence (~ 65 % of measurements), SO_2 measurements tend to be higher, but are still within standard deviation of each other (median: 0.54×10^{10} cm^{-3} (Manaus), 0.38×10^{10} cm^{-3} (no Manaus). Similarly,

200 measured H_2SO_4 differed minimally between periods with and without Manaus influence (median: 8.77×10^5 cm^{-3} (Manaus), 7.40×10^5 cm^{-3} (no Manaus), though interestingly nighttime H_2SO_4 is slightly larger when there is minimal influence from Manaus. OH measurements are about twice as large during periods with Manaus influence compared to those without (median: 2.40×10^5 cm^{-3} (Manaus), 1.24×10^5 cm^{-3} (no Manaus), and O_3 is about 1.5 times larger during periods with Manaus influence (median: 3.90×10^5 cm^{-3} (Manaus), 2.78×10^{11} cm^{-3} (no Manaus). The O_3 measurements are consistent with

205 those reported in Kuhn et al. (2010), in which aircraft measurements reported heightened levels of O_3 in air masses with Manaus emissions compared to those without. Given the frequency of Manaus influence during both IOPs, the analysis of this effect on the H_2SO_4 estimations performed in this study is discussed at the end of the results and discussion.

The concentration of H_2SO_4 was estimated using Proxy 1, which includes production from the oxidation of SO_2 by OH and loss from CS. The results of this estimation are plotted as a function of the measured H_2SO_4 in Figure 2a. Estimates

210 from IOPs 1 and 2 fall below the 1:1 line, meaning the proxy tends to underestimate measured H_2SO_4 by an average factor of 3.7. Despite a generally linear trend exhibited between the estimated and measured values, there is a weak correlation (0.46) between these two that cannot be attributed to a single parameter (CS, OH, SO_2) included in the proxy. While this proxy is advantageous in that it is the only proxy tested that depends directly on the concentrations of species that react to form H_2SO_4 and uses measured rate constants to perform estimations, in the Amazon Basin this estimation provides a lower limit

215 of H_2SO_4 concentrations. Our results further support the hypothesis that there is another source of H_2SO_4 in this region that is not described by OH initiated oxidation of SO_2. They also indicate that loss from CS may not be the only loss pathway for H_2SO_4.

To evaluate whether global radiation is a sufficient substitute for OH during daytime, we used Proxy 2 to estimate H_2SO_4. The value of k' was calculated as a fit parameter between the log of the proxy terms (GlobRad, SO_2, CS) and the log of the

220 measured H_2SO_4 for the entire data set (Fig. S2). The calculated value of k' is 2.43×10^{-10} m^2 s^1 W^{-1}, which is smaller than the fit value reported in Petäjä et al. (2009) 1.4×10^{-7} m^2 s^1 W^{-1}). The difference in k' is a result of the dependence of the proxy on radiation between the location used in this study and Hyytiälä, which was used in Petäjä et al. (2009). A drawback to this estimation compared to Proxy 1 is that it does not rely on the specific reactants that produce H_2SO_4. Figure 2b shows that this estimation, like that from Proxy 1, falls below the 1:1 line, though to an even larger degree than the first proxy ($R^2 =$
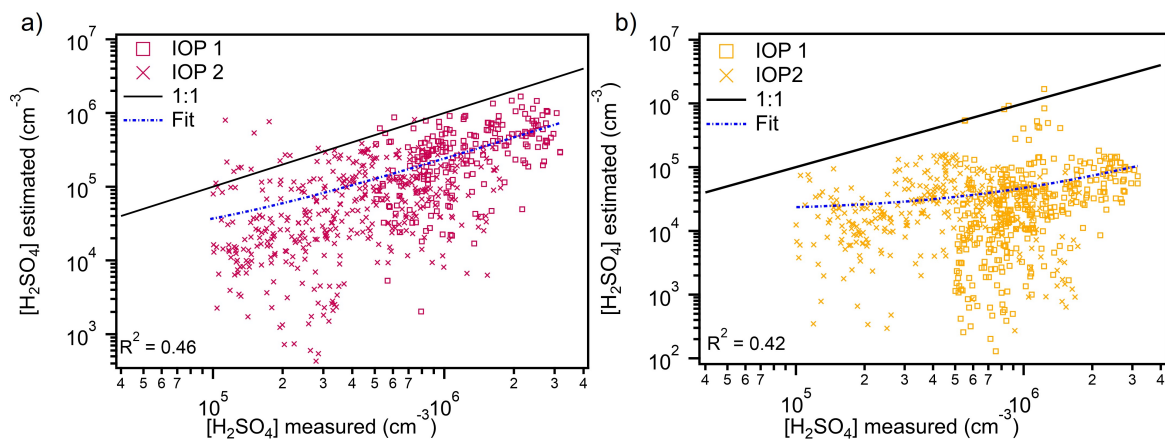
Figure 2. Estimated concentrations of sulfuric acid from Proxy 1 (865 points) (a) and Proxy 2 (1941 points) (b) versus measured concentrations. Data from IOP 1 are plotted as boxes and data from IOP 2 are plotted as crosses. The 1:1 line is plotted to guide the eye. The fit line represents the fit between the measured and proxy-estimated values of sulfuric acid.

0.42). Interestingly, the fits for both Proxy 1 and Proxy 2 have slopes of $\sim$ 40, highlighting the similar average underestimation of H_2SO_4 by both proxies. Measurements of OH and radiation show little correlation during the observation period (Fig. S3), supporting the hypothesis that secondary OH production from O_3 reaction with isoprene contributes significantly in this region (Lelieveld et al., 2008, 2016). Similar results are obtained when using the proxy reported by Petäjä et al. (2009) (Fig. S4). Both proxies do a particularly poor job estimating concentrations during IOP 2 (Fig. 2b), in which the estimates do not exhibit a trend with the measured values. This can be attributed to a lack of correlation between H_2SO_4 and radiation during this portion of the observation period (Fig. S3a).

Interestingly, the main underestimations made with Proxy 2 occur when the value of global radiation falls between 10 - 100 W m^{-2}. Previous studies have used 10 W m^{-2} (Mikkonen et al., 2011) and 50 W m^{-2} (Dada et al., 2020) as the lower cut-off for radiation, although these results indicate that increasing the lower limit for radiation to 100 W m^{-2} would likely improve estimates. Since both H_2SO_4 and OH were measured when radiation was less than 100 W m^2 throughout the entire campaign (Fig. S3), this would be at the expense of estimating H_2SO_4 during low-light (radiation < 100 W m^{-2}) conditions, when secondary production of OH is likely the dominant source of OH. This discrepancy suggests that a combination of other H_2SO_4 sources and secondary OH production are contributing to H_2SO_4 levels, which is not being accounted for in this parameterization. Further investigation into the relative importance of primary and secondary OH production pathways should be performed to determine a generalized radiation lower cut-off value for application of these general H_2SO_4 proxies during daytime hours. Additionally, more examination of the relative contributions from primary and secondary OH production pathways is necessary to evaluate how well solar radiation represents OH across a range of locations.

The best predictive proxy reported in Mikkonen et al. (2011) (Proxy 3) was also tested using the Amazon Basin data set. Like Proxy 2, this uses global radiation instead of OH, though as described earlier it was developed using measurements from
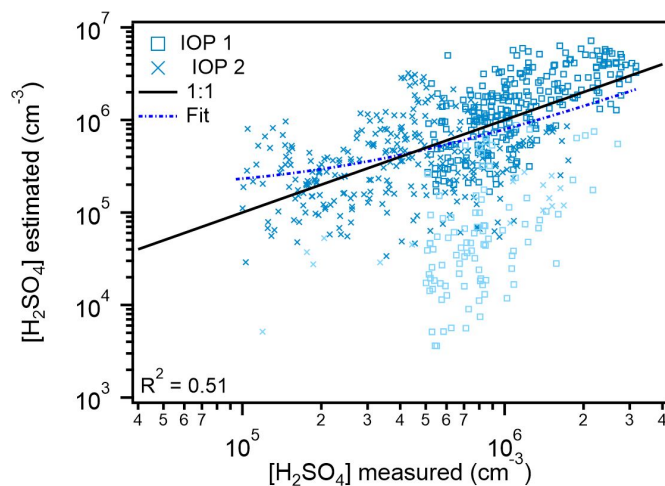
Figure 3. Estimated concentrations of sulfuric acid from Proxy 3 versus measured concentrations (1172 points). Data from IOP 1 is plotted as boxes and data from IOP 2 is plotted as crosses. Data points are color-coded to represent the amount of global radiation measured at that time; light blue points were when global radiation was 0 - 100 W m^2, and dark blue points were when global radiation exceeded 100 W m^2. The 1:1 line is plotted to guide the eye. The fit line represents the fit between the measured and proxy-estimated values of sulfuric acid.

245 a variety of different environments and has significant differences in both the H_2SO_4 source and sink terms. This proxy has a reduced dependence on SO_2 in the source term, as well as a reduced dependence on loss to particle surface area, which includes a term meant to represent particulate hygroscopic growth ($CS \cdot RH$) (Table 1). Figure 3 shows that the estimations from both IOPs fall much closer to the 1:1 line than for Proxies 1 and 2, with a particularly noticeable improvement for IOP 2 compared to Proxy 2. Unlike with Proxy 2, the estimations here for IOP 2 exhibit a trend with the measured values of H_2SO_4. The

250 lighter-colored markers represent data points where global radiation is between 10 - 100 W m^{-2}. This underestimation during these low-light conditions was also seen in the estimates from Proxy 2, further supporting the need for inclusion of secondary OH production in an effective parameterization in the Amazon Basin and more investigation into a generalized lower limit for values of radiation used in these parameterizations. These improved estimates from this proxy with reduced dependence on the concentration of SO_2 support the hypothesis reported in Mikkonen et al. (2011) that SO_2 is an indicator of particulate

255 pollution, which acts as a sink for both H_2SO_4 and OH. Additionally, the Amazon Basin is very humid (campaign average RH 89 ± 13 %) and sampled aerosols are dried to below 20 % RH before classification, so accounting for hygroscopic growth of particles in the CS term may better represent the actual particle surface area available for H_2SO_4 uptake. This can also help explain the marked improvements over estimates from Proxies 1 and 2, both of which underestimate measured H_2SO_4.

We plotted the diurnal cycle of each proxy to assess their efficacy in estimating H_2SO_4 at different times of the day (Fig.

260 4). Proxy 1, which is the only proxy to include the concentration of OH, is also the only proxy shown to include nighttime estimations of H_2SO_4. Since both species were measured at night in the Amazon Basin (Fig. 1), this illustrates a major limitation of the other proxies that use global radiation as a substitute for OH. Despite Proxy 1 providing nighttime estimates
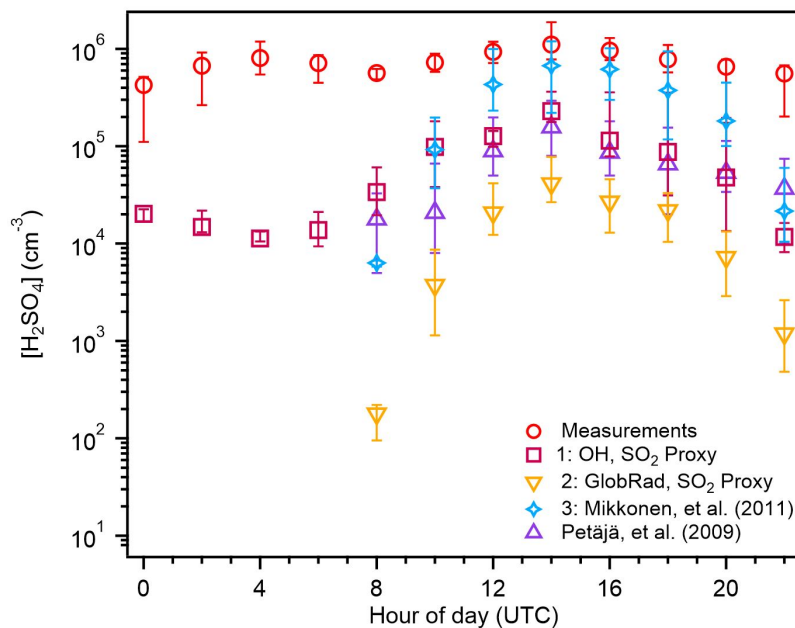
Figure 4. Two-hour averaged diurnal variation of the median sulfuric acid measurements (red), and estimations from Proxies 1 (purple), 2 (yellow), and 3 (blue) for the entire campaign. The bars represent the 25th - 75th percentiles for each measured value. Daylight hours: 08:00 - 22:00 UTC.

of H_2SO_4, it tends to under-predict measurements by an order of magnitude during these hours. When radiation exceeds 100 W m^{-2} (10:00 UTC, Fig. 1), the proxy reported by Petäjä et al. (2009), which is very similar to Proxy 2 in this work, is competitive
265 with Proxy 1 in its predictive ability, while Proxy 2 is within the 25th percentile of the Petäjä et al. (2009) estimation, and Proxy 3 underestimates the measured values by two orders of magnitude. From 12:00 - 20:00 UTC, the Mikkonen et al. (2011) proxy (Proxy 3) best estimates the measured concentrations of H_2SO_4; the median estimation falls within the 25th - 75th percentiles of the measured values. Proxy 1 and the Petäjä et al. (2009) proxy underestimate measured concentrations by one order of magnitude during this time period, while Proxy 2 underestimates by 10^1 - 10^2 molec cm^{-3}. During daylight hours,
270 Proxies 1 and 3 are sufficient estimators of H_2SO_4 while Proxy 2 drastically underestimates measurements. Only Proxy 1 can provide nighttime estimations, which are necessary in the Amazon Basin where H_2SO_4 is measured at night. This proxy is the only one tested thus far that accounts for secondary OH production.

Several new proxies reported by Dada et al. (2020) include production of H_2SO_4 through a sCI pathway, as well as an additional loss pathway due to clustering of H_2SO_4 to form new particles. This additional source of H_2SO_4 is active at
275 nighttime, so despite these proxies depending on global radiation rather than measurements of OH concentration (Proxies 4 and 5, Table 1), nighttime estimations can still be made. Based on Figure 9 of Dada et al. (2020), the proxies developed representing boreal forest and rural environments would be most appropriate to use for the Amazon Basin conditions. Of the two proxies, only the boreal (Proxy 4) includes the sCI production pathway, though both proxies include the clustering loss term. The rural

proxy (Proxy 5) can therefore be compared to Proxies 1 - 3 to evaluate the best predictive daytime parameterization for the
280   Amazon Basin.
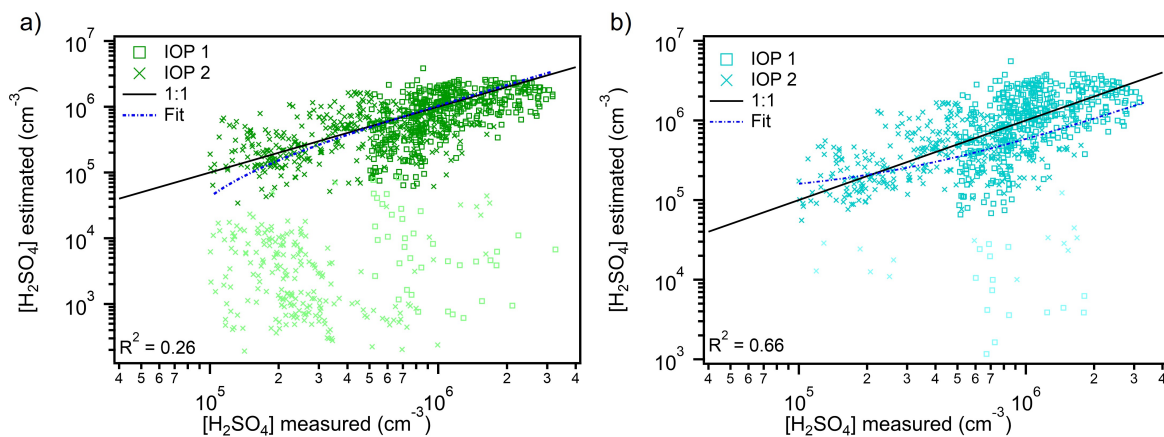
Figure 5. Estimated concentrations of sulfuric acid from Proxy 4 (1941 points) (a) and Proxy 5 (1654 points) (b) versus measured concentrations. Data from IOP 1 is plotted as boxes and data from IOP 2 is plotted as crosses. Data points are color-coded to represent the amount of global radiation measured at that time; lighter-colored points were when global radiation was 0 - 100 W m^2, and darker-colored points were when global radiation exceeded 100 W m^2. The 1:1 line is plotted to guide the eye. The fit line represents the fit between the measured and proxy-estimated values of sulfuric acid.

Figure 5a shows that data points where global radiation exceed 100 W m^{-2} from the boreal proxy (Proxy 4) fall on the 1:1 line, while those from lower-light conditions all underestimate the measured values. These underestimations (10^1 - 10^2 molec cm^{-3}) represent data points from both nighttime and twilight times of day, and are likely due to the proxy only considering the sCI formation pathway during these times. The weak correlation (0.26) between the estimated and measured values is
285   driven by the low-light data points; a much higher correlation (0.68) is achieved for data points where global radiation > 100 W m^{-2}. Since OH was measured during nighttime in the Amazon Basin, the production of H_2SO_4 from OH oxidation of SO_2 is an unaccounted for source in this estimation, and likely contributes to the low-light underestimations observed. Similar results were obtained using the combined concentrations of isoprene and monoterpene as the alkene term in this proxy (Figs. S5 and S6). Interestingly, the nighttime H_2SO_4 production term in this proxy likely also represents the main secondary OH
290   production pathway (Table 1). This illustrates the need to distinguish boreal forest environments from the tropical rainforest due to differences in OH sources; model results suggest that primary production of OH and secondary production due to NO_x are more important in the boreal forest than tropical rainforest (Lelieveld et al., 2016). The Lelieveld et al. (2016) results also indicate that even during summertime, nighttime OH is lower in the boreal forest than in the tropical rainforest. As pollution, including NOx, is expected to increase in the Amazon Basin, model results made from GoAmazon2014/5 data suggest that
295   OH levels will increase (Liu et al., 2018). Despite the similarity in many of the H_2SO_4 key predictor variables between the

Amazon Basin and Hyytiälä, there are major differences between these two locations that require consideration when using Proxy 4.

Proxy 5, which is representative of rural conditions, does not include the sCI pathway and therefore only provides daytime estimations of H_2SO_4. Data from both IOPs lie near the 1:1 line, though they have more spread around this line than the daytime

300 estimations from Proxy 4 (Fig. 5b). The few low-light data points used in this parameterization exhibit the underestimation trend seen in Proxies 3 and 4, likely due to a combination of missing the sCI H_2SO_4 source and secondary OH production like Proxy 3. There is a clear improvement in the predictive strength of this estimation compared to Proxy 1, which almost entirely underestimates measured concentrations of H_2SO_4 (Fig. 2a).

Both of the Dada et al. (2020) proxies have a higher correlation with measured H_2SO_4 when global radiation exceeds

305 100 W m^{-2} (Fig. 5) than the other radiation-based proxies (Fig. 3 and 4). This suggests that Proxies 4 and 5 should have daytime estimations that are more consistent with the Amazon Basin measurements than the previous proxies. Additionally, Proxy 4 should provide estimates during all hours of the day. Considering the amount of OH measured at nighttime during the campaign, as well as the underestimation of H_2SO_4 during low-light hours by Proxy 4, we decided to assess the efficacy of Proxy 4 if measurements of OH were substituted for global radiation in Proxy 4. We also re-fitted the coefficients of Proxy 4

310 (new Proxy shown in Eqn. 2, the results of which are shown in Figure 6.
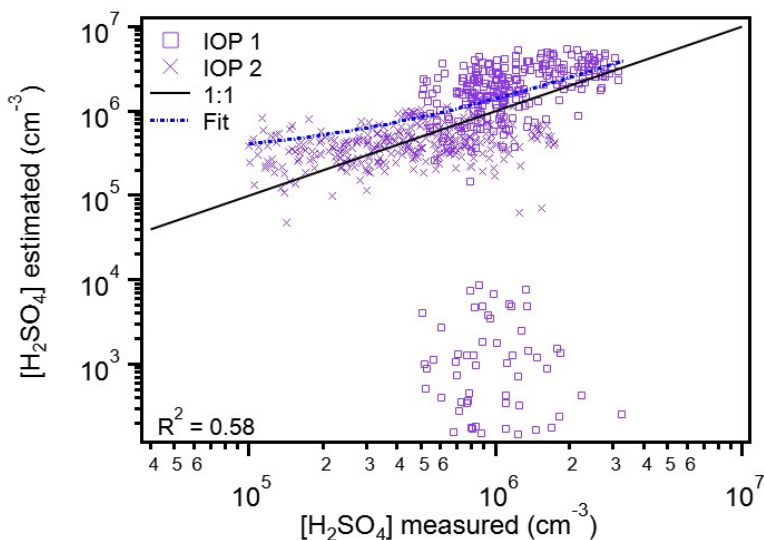
Figure 6. Estimated concentrations of sulfuric acid from Proxy 4 (8124 points), where measured OH is used instead of global radiation, versus measured concentrations. Data from IOP 1 is plotted as boxes and data from IOP 2 is plotted as crosses. The proxy coefficients were refitted and are shown in Eqn. 2. The 1:1 line is plotted to guide the eye. The fit line represents the fit between the measured and proxy-estimated values of sulfuric acid.

$$[H_2SO_4] = \frac{CS}{2 \cdot (3.6 \ x \ 10^{-8})} + \left[\left(\frac{CS}{2 \cdot (3.6 \ x \ 10^{-8})} \right)^2 + \frac{SO_2}{3.6 \ x \ 10^{-8}} \left(6.4 \ x \ 10^{-10} \cdot [OH] + 4.5 \ x \ 10^{-29} [O_3][Alkene] \right) \right]^{\frac{1}{2}}$$

(2)

As seen in Figure 6, substituting measured OH for global radiation in Proxy 4 results in estimations that are much closer to the 1:1 line. Additionally, it almost entirely eliminates the low-light underestimations shown for both IOP 1 and IOP 2 in Figure 5. There is still a large underestimation mode seen in Figure 6 for IOP 1, which like that seen in Figure 5b, corresponds 315 to a period of both low global radiation and low OH. While this underestimation contributes to the lower correlation value ($R^2 = 0.58$), overall there is much better agreement between the new Proxy 4 estimates and those made using global radiation, likely because of the better estimates under low-light conditions. To test this hypothesis, the diurnal cycles of these proxies and the measurements of H_2SO_4 were plotted for comparison.
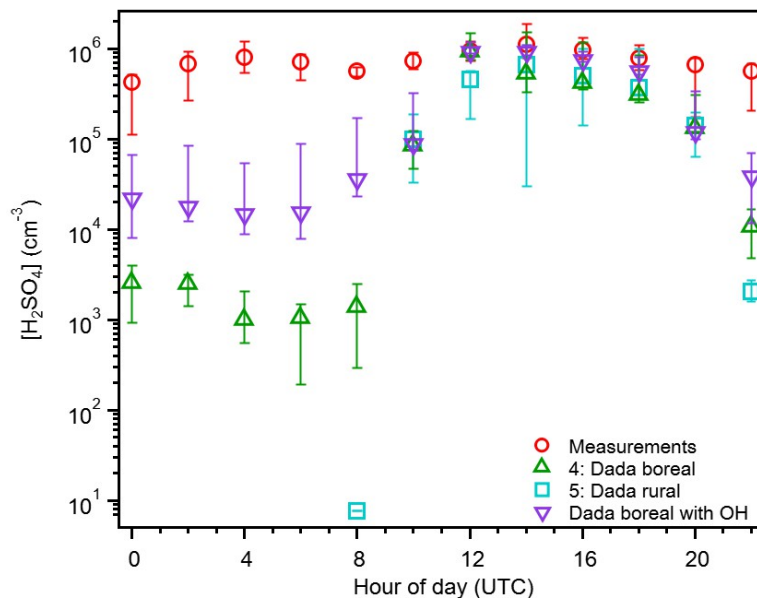
Figure 7. Two-hour averaged diurnal variation of the median sulfuric acid measurements (red), and estimations from Proxies 4 (green), 5 (teal), and Eqn. 2 (purple) for the entire campaign. The bars represent the 25th - 75th percentiles for each value. Daylight hours: 08:00 - 22:00 UTC.

As hypothesized, the estimations from 12:00 - 20:00 UTC for Proxy 4 and 14:00 - 20:00 UTC for Proxy 5 are within the 320 25th - 75th percentile bars of the H_2SO_4 measurements (Fig. 7). Both estimations at 10:00 UTC are similar to those from Proxies 1 and 3, and all four estimate more accurately than Proxy 2 and the Petäjä et al. (2009) proxy (Fig. 4). The consistency between Proxies 3 and 5 during daylight hours indicates that the clustering of H_2SO_4 molecules to form new atmospheric

particles is not a major loss source during this time of day. The boreal proxy (Proxy 4) greatly underestimates measurements at nighttime (10^2 molec cm^{-3}), and are one order of magnitude smaller than those from Proxy 1 (Fig. 4). In order to match

325 the concentrations of H_2SO_4 measured between 0:00 - 8:00 UTC, there would need to be an increase of 10^3 molec cm^{-3} of alkene (median concentration necessary: 2.9×10^{12} molec cm^3), which is larger than the total concentration of monoterpenes and isoprene measured during the campaign (Fig. S6). Substituting OH for global radiation in the boreal proxy, resulting in the parameterization described by Equation 2, significantly improves these estimates during nighttime hours. However, the underestimation of measurements seen in this proxy at night is likely reflective of the parameterizations not including non-

330 SO_2 sources of sulfur. These results suggest that both the sCI and OH oxidation of SO_2 are contributors at nighttime in the Amazon Basin, and perhaps in other locations as well. Estimating H_2SO_4 concentrations at night is currently the main area of uncertainty with current proxies, and while measurements of OH are difficult to make, they are key to determining low-light and nighttime sources of H_2SO_4 for developing a robust proxy for general use.

The modified boreal proxy from Dada et al. (2020) (Eqn. 2) is the best general use proxy for the Amazon Basin. This proxy

335 provides the most representative estimations of H_2SO_4, considering both overall estimations (Fig. 6) and the diurnal cycle compared to measured values (Fig. 7). Though the Mikkonen et al. (2011), boreal, and rural proxies provide similarly accurate estimations during daylight hours and Proxy 4 provides nighttime estimates, substituting OH for global radiation (Eqn. 2) provides the most accurate nighttime estimations. Our results support the Dada et al. (2020) recommendation to compare a given location's conditions to those reported in Figure 9 of that work to determine the most appropriate proxy to use. The

340 conditions in the Amazon Basin best aligned with the boreal conditions reported in that work, and of the currently published parameterizations tested, that proxy provided the best estimates of H_2SO_4. We note that caution should be applied to estimates from this parameterization due to differences in OH production pathways between the boreal forest and tropical rainforest environments, and recommend substituting OH concentration for global radiation in Proxy 4, and refitting the coefficients in that equation when OH measurements are available. These results support the inclusion of the sCI production pathway and

345 loss due to clustering pathway in a robust proxy. They also show that replacing the concentration of OH with global radiation is insufficient for proxies in the Amazon Basin where OH has been measured at nighttime (Fig. 1), and likely contributes to the measured H_2SO_4 during this time of day. For estimations of solely daytime concentrations of H_2SO_4 (global radiation > 100 W m^{-2}), the Dada et al. (2020) estimations (Proxies 4 and 5) and Mikkonen et al. (2011) parameterization (Proxy 3) provide the best estimations of H_2SO_4 (Fig. 3-7). These proxies provide better daytime estimations than the photochemical

350 proxies that only consider production of H_2SO_4 via OH oxidation of SO_2, and loss solely to particle surface area (CS). As expected by the higher concentrations of OH and O_3 measured in periods without Manaus influence, Proxies 1 and 4 provided better estimations of H_2SO_4 when the site experienced influence from Manaus (Fig. S8). In particular, the nighttime estimating power of these proxies is much improved (by ~ 10 cm^{-3}), suggesting that anthropogenic influence contributes to the nighttime sources of H_2SO_4 in this region.

4 Conclusions

This paper reports, to the best of our knowledge, the first measurements of H_2SO_4 from the Amazon Basin. The median concentrations measured during both the wet (IOP 1: 7.82×10^5 molec cm^{-3}) and dry (IOP 2: 2.59×10^5 molec cm^{-3}) seasons differed only slightly from each other, indicating that seasonal changes have minimal impact on H_2SO_4 in this region. These concentrations are consistent with measured values from the boreal forest in Hyytiälä (Dada et al., 2020; Mikkonen et al., 2011), and much lower than measurements from more urban locations (Dada et al., 2020; Mikkonen et al., 2011). Our results show minimal diurnal variation across both seasons and no clear correlation with global radiation, in contrast previous measurements of H_2SO_4 from a variety of locations (Dada et al., 2020; Mikkonen et al., 2011; Petäjä et al., 2009). These results suggest that photochemical oxidation of SO_2 by OH is not the only source of H_2SO_4 in the region, as well as demonstrate the importance of including measurements from a wide range of sites to develop a general-use H_2SO_4 proxy.

The best predictive proxy for all light conditions was the boreal proxy reported in Dada et al. (2020)with OH substituted for global radiation, though the published proxy using global radiation was the second-best tested here. This was the only radiation-dependent proxy to provide nighttime estimations, which is a clear advantage for use in an environment like this one where there is measurable nighttime H_2SO_4. If nighttime estimations of H_2SO_4 are necessary for environments similar to the Amazon Basin, the boreal proxy reported in Dada et al. (2020) is the best available estimation for low-light data when measurements of OH are unavailable. However, we note that the nighttime estimations are incomplete because the production via OH oxidation of SO_2 is not included, and including measurements of OH in this parameterization improved nighttime estimates of H_2SO_4. Additionally, this parameterization does not include a sink for Criegee intermediates, which may be important in this region with high RH. The validity of the rural proxy from Dada et al. (2020) and the best proxy from Mikkonen et al. (2011) are supported for daytime estimations (radiation > 100 W m^{-2}) by these results. All four provide estimations within the 25th to 75th percentile of the measured concentrations under these conditions.

Based on the measurements from the Amazon Basin and the proxy results, both the sCI and SO_2 oxidation by OH pathways for H_2SO_4 production contribute during low-light and nighttime conditions. This combination under low-light conditions is not currently accounted for by any existing H_2SO_4 proxy, and may be responsible for low-light H_2SO_4 in other tropical and low-NO_x environments. The combination of biogenic emissions from the rain forest combined with fresh anthropogenic emissions from local farms and aged anthropogenic emissions from Manaus provides more chemical heterogeneity than what is observed in Hyytiälä (Asmi et al., 2011; Dada et al., 2017; Kulmala et al., 2016), which may help explain the observed discrepancy between the measured and estimated H_2SO_4 concentrations. More measurements from the Southern Hemisphere, which has lower NO_x compared to the Northern Hemisphere, should be used to test and construct H_2SO_4 proxies to more accurately represent the variety of H_2SO_4 and OH sources.

These results, which are the first to test existing proxies using data from the Southern Hemisphere, demonstrate the challenges in simplifying the complex processes controlling H_2SO_4 levels into an equation. We observed that radiation is not always an effective substitute for OH concentrations, particularly when global radiation is between 0 - 100 W m^{-2}. This substitution is not valid in locations where there is measurable OH at night, due to production from secondary sources such as

O_3 oxidation of alkenes like isoprene. While OH is difficult to measure, effort should be made to collect more measurements across a variety of environments to assess its contribution to the H_2SO_4 population during low-light and nighttime conditions, to help develop proxies that more accurately account for this nighttime chemistry. In particular, more OH measurements are needed in the Southern Hemisphere to constrain OH models and improve H_2SO_4 parameterizations.

Data availability. GoAmazon2014/5 data used in this study are available from the ARM website: https://doi.org/10.5439/1346559 (ARM, 2022).

Author contributions. Measurements were made by SK, SS, AG, RS, OVB, JT, RAFS, and JS. DM performed proxy estimations, and DM and JS helped analyze results. DM prepared the manuscript with contributions from SK, SS, AG, RS, OVB, JT, RAFS, and JS.

Competing interests. The authors declare that they have no conflicts of interest.

Acknowledgements. Institutional support for GoAmazon2014/5 was provided by the Central Office of the Large Scale Biosphere Atmosphere Experiment in Amazonia (LBA), the National Institute of Amazonian Research (INPA), and Amazonas State University (UEA) and the local Research Support Foundation (FAPEAM/GOAMAZON). We also acknowledge support from the Atmospheric Radiation Measurement (ARM) Climate Research Facility, a user facility of the United States Department of Energy, Office of Science, sponsored by the Office of Biological and Environmental Research, and support from the Atmospheric System Research (ASR, DE-SC0011122 and DE-SC0011115) program of that office. JS acknowledges support from a Brazilian Science Mobility Program (Programa Ciência sem Fronteiras) Special Visiting Researcher Scholarship. RS acknowledges grants RYC2020-029216-I and CEX2018-000794-S funded by MCIN/AEI/ 10.13039/501100011033 and by "ESF Investing in your future". The authors would also like to thank Michelia Dam, Hayley Glicker, Adam Thomas, and Jeremy Wakeen for their contributions to discussions regarding this project.

References

Almeida, J., Schobesberger, S., Kürten, A., Ortega, I. K., Kupiainen-Määttä, O., Praplan, A. P., Adamov, A., Amorim, A., Bianchi, F., Breitenlechner, M., , David, A., Dommen, J., Donahue, N. M., Downard, A., Dunne, E., Duplissy, J., Ehrhart, S., Flagan, R. C., Franchin, A., Guida, R., Hakala, J., Hansel, A., Heinritzi, M., Henschel, H., Jokinen, T., Junninen, H., Kajor, M., Kangasluoma, J., Keskinen, H., Kupc, A., Kurtén, T., Kvashin, A. N., Laaksonen, A., Lehtipalo, K., Leiminger, M., Leppä, J., Louonen, V., Makhmutov, V., Mathot, S., McGrath, M. J., Nieminen, T., Olenius, T., Onnela, A., Petäjä, T., Riccobono, F., Riipinen, I., Rissanen, M., Rondo, L., Ruuskanen, T., Santos, F. D., Sarnela, N., Schallhart, S., Schnitzhofer, R., Seinfeld, J. H., Simon, M., Sipilä, M., Stozhkov, Y., Stratmann, F., Tomé, A., Tröstl, J., Tragkogeorgas, G., Vaatovaara, P., Viisanen, Y., Virtanen, A., Vrtala, A., Wagner, P. E., Weingartner, E., Wex, H., Williamson, C., Wimmer, D., Ye, P., Yli-Juuti, T., Carslaw, K. S., Kulmala, M., Curtius, J., Baltensperger, U., Worsnop, D. R., Vehkamä, H., and Kirkby, J.: Molecular Understanding of Sulphuric Acid–Amine Particle Nucleation in the Atmosphere, Nature, 502, 359–363, https://doi.org/10.1038/nature12663, 2013.

Andreae, M. O. and Andreae, T. W.: The cycle of biogenic sulfur compounds over the Amazon Basin: 1. Dry season, Journal of Geophysical Research: Atmospheres, 93, 1487–1497, https://doi.org/10.1029/JD093ID02P01487, 1988.

Andreae, M. O., Berresheim, H., Bingemer, H., Jacob, D. J., Lewis, B. L., Li, S. M., and Talbot, R. W.: The atmospheric sulfur cycle over the Amazon Basin: 2. Wet season, Journal of Geophysical Research: Atmospheres, 95, 16 813–16 824, https://doi.org/10.1029/JD095ID10P16813, 1990.

Andreae, M. O., Rosenfeld, D., Artaxo, P., Costa, A. A., Frank, G. P., Longo, K. M., and Silva-Dias, M. A. F.: Smoking Rain Clouds over the Amazon, Science, 303, 1337–1342, https://doi.org/10.1126/science.1092779, 2004.

ARM: Atmospheric Radiation Measurement (ARM) user facility. 2014, updated hourly. Surface Meteorological Instrumentation (MET). 2014-02-09 to 2014-10-01, ARM Mobile Facility (MAO) Manacapuru, Amazonas, Brazil; AMF1 (M1). Compiled by J. Kyrouac and D. Holdridge, https://doi.org/10.5439/1025220, 2014a.

ARM: Atmospheric Radiation Measurement (ARM) user facility, 2014, updated hourly. Sky Radiometers on Stand for Downwelling Radiation (SKYRAD60S), 2014-02-09 to 2014-10-01, ARM Mobile Facility (MAO) Manacapuru, Amazonas, Brazil; AMF1 (M1). Compiled by M. Sengupta, https://doi.org/10.5439/1025281, 2014b.

ARM: Atmospheric Radiation Measurement (ARM) Climate Research Facility, 2014, updated hourly, Scanning mobility particle sizer (AOSSMPS). 2014-03-13 to 2014-03-24, ARM Mobile Facility (MAO), https://adc.arm.gov/discovery/#/results/instrument_class_code:: smps/site_code::mao/start_date::2014-01-01/end_date::2015-11-30, 2014c.

ARM: Campaign Datasets for Observations and Modeling of the Green Ocean Amazon (GoAmazon), last accessed 2 February 2022, https://doi.org/10.5439/1346559, 2022.

Artaxo, P., Rizzo, L. V., Brito, J. F., Barbosa, H. M., Arana, A., Sena, E. T., Cirino, G. G., Bastos, W., Martin, S. T., and Andreae, M. O.: Atmospheric aerosols in Amazonia and land use change: From natural biogenic to biomass burning conditions, Faraday Discussions, 165, 203–235, https://doi.org/10.1039/c3fd00052d, 2013.

Asmi, A., Wiedensohler, A., Laj, P., Fjaeraa, A. M., Sellegri, K., Birmili, W., Weingartner, E., Baltensperger, U., Zdimal, V., Zikova, N., Putaud, J. P., arinoni, A., Tunved, P., Hansson, H. C., Fiebig, M., Kivekäs, N., Lihavainen, H., Asmi, E., Ulevicius, V., Aalto, P. P., Swietlicki, E., Kristensson, A., Mihalopoulos, N., Kalivitis, N., Kalapov, I., Kiss, G., De Leeuw, G., Henzing, B., Harrison, R. M., Beddows, D., O'Dowd, C., Jennings, S. G., Flentje, H., Weinhold, K., Meinhardt, F., Ries, L., and Kulmala, M.: Number size distributions and sea-

sonality of submicron particles in Europe 2008-2009, Atmospheric Chemistry and Physics, 11, 5505–5538, https://doi.org/10.5194/ACP-11-5505-2011, 2011.

445 Bzdek, B. R., Zordan, C. A., Pennington, M. R., Luther, G. W., and Johnston, M. V.: Sources and sinks driving sulfuric acid concentrations in contrasting environments: Implications on proxy calculations, Environmental Science and Technology, 46, 4365–4373, https://doi.org/10.1021/es204556c, 2012.

Dada, L., Paasonen, P., Nieminen, T., Buenrostro Mazon, S., Kontkanen, J., Peräkylä, O., Lehtipalo, K., Hussein, T., Petäjä, P., Kerminen, V.-M., Bäck, J., and Kulmala, M.: Long-term analysis of clear-sky new particle formation events and nonevents in Hyytiälä, Atmospheric

450 Chemistry and Physics, 17, 6227–6241, https://doi.org/10.5194/ACP-17-6227-2017, 2017.

Dada, L., Ylivinkka, I., Baalbaki, R., Li, C., Guo, Y., Yan, C., Yao, L., Sarnela, N., Jokinen, T., Daellenbach, K. R., Yin, R., Deng, C., Chu, B., Nieminen, T., Wang, Y., Li, Z., Thakur, R. C., Kontkanen, J., Stolzenburg, D., Sipilä, M., Hussein, T., Paasonen, P., Bianchi, F., Salma, I., T., W., Pikridas, M., Sciare, J., Jiang, J. Liu, Y., Petä, jä, P., Kermimen, V.-M., and Kulmala, M.: Sources and sinks driving sulfuric acid concentrations in contrasting environments: Implications on proxy calculations, Atmospheric Chemistry and Physics, 20, 11 747–11 766,

455 https://doi.org/10.5194/acp-20-11747-2020, 2020.

DeMore, W., Howard, C., Sander, S., Ravishankara, A., Golden, D., Kolb, C., Hampson, R., Molina, M., and Kurylo, M.: Chemical Kinetics and Photochemical Data for Use in Stratospheric Modeling Evaluation Number 12 NASA Panel for Data Evaluation, Jet Propulsion Laboratory, California Institute of Technology, 1997.

Dunne, E. M., Gordon, H., Kürten, A., Almeida, J., Duplissy, J., Williamson, C., Ortega, I. K., Pringle, K. J., Adamov, A., Baltensperger,

460 U., Barmet, P., Benduhn, F., Bianchi, F., Breitenlechner, M., Clarke, A., Curtius, J., Dommen, J., Donahue, N. M., Ehrhart, S., Flagan, R. C., Franchin, A., Guida, R., Hakala, J., Hansel, A., Heinritzi, M., Jokinen, T., Kangasluoma, J., Kirkby, J., Kulmala, M., Kupc, A., Lawler, M. J., Lehtipalo, K., Makhmutov, V., Mann, G., Mathot, S., Merikanto, J., Miettinen, P., Nenes, A., Onnela, A., Rap, A., Reddington, C. L., Riccobono, F., Richards, N. A., Rissanen, M. P., Rondo, L., Sarnela, N., Schobesberger, S., Sengupta, K., Simon, M., Sipilä, M., Smith, J. N., Stozhkov, Y., Tomé, A., Tröstl, J., Wagner, P. E., Wimmer, D., Winkler, P. M., Worsnop,

465 D. R., and Carslaw, K. S.: Global atmospheric particle formation from CERN CLOUD measurements, Science, 354, 1119–1124, https://doi.org/10.1126/SCIENCE.AAF2649/SUPPL_FILE/PAPV3.PDF, 2016.

Eisele, F. L. and Bradshaw, J. D.: The elusve hydroxyl radical: measuring OH in the atmosphere, Analytical Chemistry, 65, 927–939, https://doi.org/10.1021/ac00069a723, 1993.

Fiedler, V., Dal Maso, M., Boy, M., Aufmhoff, H., Hoffmann, J., Schuck, T., Birmili, W., Hanke, M., Uecker, J., Arnold, F., and Kulmala,

470 M.: The contribution of sulphuric acid to atmospheric particle formation and growth: A comparison between boundary layers in Northern and Central Europe, Atmospheric Chemistry and Physics, 5, 1773–1785, https://doi.org/10.5194/acp-5-1773-2005, 2005.

Glicker, H. S., Lawler, M. J., Ortega, J., De Sá, S. S., Martin, S. T., Artaxo, P., Vega Bustillos, O., De Souza, R., Tota, J., Carlton, A., and Smith, J. N.: Chemical composition of ultrafine aerosol particles in central Amazonia during the wet season, Atmospheric Chemistry and Physics, 19, 13 053–13 066, https://doi.org/10.5194/acp-19-13053-2019, 2019.

475 Gordon, H., Kirkby, J., Baltensperger, U., Bianchi, F., Breitenlechner, M., Curtius, J., Dias, A., Dommen, J., Donahue, N. M., Dunne, E. M., Duplissy, J., Ehrhart, S., Flagan, R. C., Frege, C., Fuchs, C., Hansel, A., Hoyle, C. R., Kulmala, M., Kürten, A., Lehtipalo, K., Makhmutov, V., Molteni, U., Rissanen, M. P., Stozhkov, Y., Tröstl, J., Tsagkogeorgas, G., Wagner, R., Williamson, C., Wimmer, D., Winkler, P. M., Yan, C., and Carslaw, K. S.: Causes and importance of new particle formation in the present-day and preindustrial atmospheres, Journal of Geophysical Research: Atmospheres, 122, 8739–8760, https://doi.org/10.1002/2017JD026844, 2017.

480 Jen, C. N., Bachman, R., Zhao, J., McMurry, P. H., and Hanson, D. R.: Diamine-sulfuric acid reactions are a potent source of new particle formation, Geophysical Research Letters, 43, 867–873, https://doi.org/10.1002/2015GL066958, 2016.

Jeong, D., Seco, R., Emmons, L., Schwantes, R., Liu, Y., McKinney, K. A., Martin, S. T., Keutsch, F. N., Gu, D., Guenther, A. B., Vega, O., Tota, J., Souza, R. A. F., Springston, S. R., Watson, T. B., and Kim, S.: Reconciling Observed and Predicted Tropical Rainforest OH Concentrations, Journal of Geophysical Research: Atmospheres, 127, https://doi.org/10.1029/2020JD032901, 2022.

485 Jokinen, T., Sipilä, M., Junninen, H., Ehn, M., Lönn, G., Hakala, J., Petäjä, T., Mauldin, R. L., Kulmala, M., and Worsnop, D. R.: Atmospheric sulphuric acid and neutral cluster measurements using CI-APi-TOF, Atmospheric Chemistry and Physics, 12, 4117–4125, https://doi.org/10.5194/ACP-12-4117-2012, 2012.

Kerminen, V. M., Paramonov, M., Anttila, T., Riipinen, I., Fountoukis, C., Korhonen, H., Asmi, E., Laakso, L., Lihavainen, H., Swietlicki, E., Svenningsson, B., Asmi, A., Pandis, S. N., Kulmala, M., and Petäjä, T.: Cloud condensation nuclei production associated with at-
490 mospheric nucleation: A synthesis based on existing literature and new results, Atmospheric Chemistry and Physics, 12, 12 037–12 059, https://doi.org/10.5194/ACP-12-12037-2012, 2012.

Korhonen, P., Kulmala, M., Laaksonen, A., Viisanen, Y., McGraw, R., and Seinfeld, J. H.: Ternary nucleation of H2SO4, NH3, and H2O in the atmosphere, Journal of Geophysical Research Atmospheres, 104, 26 349–26 353, https://doi.org/10.1029/1999jd900784, 1999.

Kuang, C.: Scanning Mobility Particle Sizer Spectrometer Instrument Handbook, DOE/SC-ARM-TR-179, 2016.

495 Kuang, C., Riipinen, I., Sihto, S.-L., Kulmala, M., McCormick, A. V., and McMurry, P. H.: An improved criterion for new particle formation in diverse atmospheric environments, Atmospheric Chemistry and Physics, 10, 8469–8480, https://doi.org/10.5194/acp-10-8469-2010, 2010.

Kuhn, U., Ganzeveld, L., Thielmann, A., Dindorf, T., Schebeske, G., Welling, M., Sciare, J., Roberts, G., Meixner, F. X., Kesselmeier, J., Lelieveld, J., Kolle, O., Ciccioli, P., Lloyd, J., Trentmann, J., Artaxo, P., and Andreae, M. O.: Impact of Manaus City on the Amazon
500 Green Ocean atmosphere: Ozone production, precursor sensitivity and aerosol load, Atmospheric Chemistry and Physics, 10, 9251–9282, https://doi.org/10.5194/ACP-10-9251-2010, 2010.

Kulmala, M., Dal Maso, M., Mäkelä, J. M., Pirjola, L., Väkevä, M., Aalto, P., Miikkulainen, P., Hämeri, K., and O'Dowd, C. D.: On the formation, growth and composition of nucleation mode particles, Tellus, Series B: Chemical and Physical Meteorology, 53, 479–490, https://doi.org/10.3402/tellusb.v53i4.16622, 2001.

505 Kulmala, M., Vehkamäki, H., Petäjä, T., Dal Maso, M., Lauri, A., Kerminen, V. M., Birmili, W., and McMurry, P. H.: Formation and growth rates of ultrafine atmospheric particles: A review of observations, Journal of Aerosol Science, 35, 143–176, https://doi.org/10.1016/j.jaerosci.2003.10.003, 2004.

Kulmala, M., Petäjä, T., Nieminen, T., Sipilä, M., Manninen, H. E., Lehtipalo, K., Dal Maso, M., Aalto, P. P., Junninen, H., Paasonen, P., Riipinen, I., Lehtinen, K., Laaksonen, A., and Keriminen, V.-M.: Measurement of the nucleation of atmospheric aerosol particles, Nature
510 Protocols, 7, 1651–1667, https://doi.org/10.1038/nprot.2012.091, 2012.

Kulmala, M., Hämeri, K., Aalto, P. P., Mäkelä, J. M., Pirjola, L., Nilsson, E. D., Buzorius, G., Rannik, Ü., Dal Maso, M., Seidl, W., Hoffman, T., Janson, R., Hansson, H. C., Viisanen, Y., Laaksonen, A., and O'Dowd, C. D.: Overview of the international project on biogenic aerosol formation in the boreal forest (BIOFOR), http://dx.doi.org/10.3402/tellusb.v53i4.16601, 53, 324–343, https://doi.org/10.3402/TELLUSB.V53I4.16601, 2016.

515 Lelieveld, J., Butler, T. M., Crowley, J. N., Dillon, T. J., Fischer, H., Ganzeveld, L., Harder, H., Lawrence, M. G., Martinez, M., Taraborrelli, D., and Williams, J.: Atmospheric oxidation capacity sustained by a tropical forest, Nature 2008 452:7188, 452, 737–740, https://doi.org/10.1038/nature06870, 2008.

Lelieveld, J., Gromov, S., Pozzer, A., and Taraborrelli, D.: Global tropospheric hydroxyl distribution, budget and reactivity, Atmos. Chem. Phys, 16, 12 477–12 493, https://doi.org/10.5194/acp-16-12477-2016, 2016.

520 Liu, Y., Seco, R., Kim, S., Guenther, A. B., Goldstein, A. H., Keutsch, F. N., Springston, S. R., Watson, T. B., Artaxo, P., Souza, R. A., McKinney, K. A., and Martin, S. T.: Isoprene photo-oxidation products quantify the effect of pollution on hydroxyl radicals over Amazonia, Science Advances, 4, https://doi.org/10.1126/SCIADV.AAR2547/SUPPL_FILE/AAR2547_SM.PDF, 2018.

Lu, Y., Yan, C., Fu, Y., Chen, Y., Liu, Y., Yang, G., Wang, Y., Bianchi, F., Chu, B., Zhou, Y., Yin, R., Baalbaki, R., Garmash, O., Deng, C., Wang, W., Liu, Y., Petäjä, P., Kerminen, V.-M., Jiang, J., Kulmala, M., and Wang, L.: A proxy for atmospheric daytime gaseous sulfuric

525 acid concentration in urban Beijing, Atmospheric Chemistry and Physics, 19, 1971–1983, https://doi.org/10.5194/acp-19-1971-2019, 2019.

Martin, S., Andreae, M. O., Artaxo, P., Baumgardner, D., Chen, Q., Goldstein, A. H., Guenther, A., Heald, C. L., Mayol-Bracero, O. L., McMurry, P. H., Pauliquevis, T., Pöschl, U., Prather, K. A., Roberts, G. C., Saleska, S. R., Silva Dias, M. A., Spracklen, D. V., Swietlicki, E., and Trebs, I.: Sources and properties of Amazonian aerosol particles, Reviews of Geophysics, 48, https://doi.org/10.1029/2008RG000280,

530 2010.

Martin, S. T., Artaxo, P., MacHado, L. A., Manzi, A. O., Souza, R. A., Schumacher, C., Wang, J., Andreae, M. O., Barbosa, H. M., Fan, J., Fishc, G., Goldstein, A., Guenther, A., Jimenez, J., Pöschl, U., Silva Dias, M., Smith, J., and Wendisch, M.: Introduction: Observations and Modeling of the Green Ocean Amazon (GoAmazon2014/5), Atmospheric Chemistry and Physics, 16, 4785–4797, https://doi.org/10.5194/acp-16-4785-2016, 2016.

535 Mauldin, R. L., Frost, G. J., Chen, G., Tanner, D. J., Prevot, A. S. H., Davis, D. D., and Eisele, F. L.: OH measurements during the First Aerosol Characterization Experiment (ACE 1): Observations and model comparisons, Journal of Geophysical Research: Atmospheres, 103, 16 713–16 729, https://doi.org/10.1029/98JD00882, 1998.

Mauldin, R. L., Berndt, T., Sipilä, M., Paasonen, P., Petäjä, T., Kim, S., Kurtén, T., Stratmann, F., Kerminen, V. M., and Kulmala, M.: A new atmospherically relevant oxidant of sulphur dioxide, Nature, 488, 193–196, https://doi.org/10.1038/nature11278, 2012.

540 McMurry, P. H., Woo, K. S., Weber, R., Chen, D. R., and Pui, D. Y.: Size distributions of 3-10 nm atmospheric particles: Implications for nucleation mechanisms, Philosophical Transactions of the Royal Society A: Mathematical, Physical and Engineering Sciences, 358, 2625–2642, https://doi.org/10.1098/rsta.2000.0673, 2000.

Mikkonen, S., Romakkaniemi, S., Smith, J. N., Korhonen, H., Petäjä, T., Plass-Duelmer, C., Boy, M., McMurry, P. H., Lehtinen, K. E., Joutsensaari, J., HAmed, A., Mauldin, R., Birmili, W., Spindler, G., Arnold, F., Kulmala, M., and Laaksonen, A.: A statistical proxy for

545 sulphuric acid concentration, Atmospheric Chemistry and Physics, 11, 11 319–11 334, https://doi.org/10.5194/acp-11-11319-2011, 2011.

Myllys, N., Chee, S., Olenius, T., Lawler, M., and Smith, J.: Molecular-Level Understanding of Synergistic Effects in Sulfuric Acid-Amine-Ammonia Mixed Clusters, Journal of Physical Chemistry A, 123, 2420–2425, https://doi.org/10.1021/acs.jpca.9b00909, 2019.

Nobre, C. A., Sampaio, G., Borma, L. S., Castilla-Rubio, J. C., Silva, J. S., and Cardoso, M.: Land-use and climate change risks in the amazon and the need of a novel sustainable development paradigm, Proceedings of the National Academy of Sciences of the United States

550 of America, 113, 10 759–10 768, https://doi.org/10.1073/pnas.1605516113, 2016.

Paasonen, P., Nieminen, T., Asmi, E., Manninen, H. E., Petäjä, T., Plass-D ¨ Ulmer, C., Flentje, H., Birmili, W., Wiedensohler, A., Hõrrak, U., Metzger, A., Hamed, A., Laaksonen, A., M., F., Kerminen, V.-M., and Kulmala, M.: On the roles of sulphuric acid and low-volatility organic vapours in the initial steps of atmospheric new particle formation, Atmospheric Chemistry and Physics, 10, 11 223–11 242, https://doi.org/10.5194/acp-10-11223-2010, 2010.

555   Petäjä, T., Mauldin, R. L., Kosciuch, E., McGrath, J., Nieminen, T., Paasonen, P., Boy, M., Adamov, A., Kotiaho, T., and Kulmala, M.: Sulfuric acid and OH concentrations in a boreal forest site, Atmospheric Chemistry and Physics, 9, 7435–7448, https://doi.org/10.5194/acp-9-7435-2009, 2009.

Pöschl, U., Martin, S. T., Sinha, B., Chen, Q., Gunthe, S. S., Huffman, J. A., Borrmann, S., Farmer, D. K., Garland, R. M., Helas, G., and et al.: Rainforest aerosols as biogenic nuclei of clouds and precipitation in the Amazon, Science, 329, 1513–1516,
560   https://doi.org/10.1126/science.1191056, 2010.

Riipinen, I., Sihto, S.-L., Kulmala, M., Arnold, F., Dal Maso, M., Birmili, W., Saarnio, K., Teinilä, K., Kerminen, V.-M., Laaksonen, A., and Lehtinen, K.: Connections between atmospheric sulphuric acid and new particle formation during QUEST III-IV campaigns in Heidelberg and Hyytiälä, Atmospheric Chemistry and Physics, 7, 1899–1914, https://doi.org/10.5194/acp-7-1899-2007, 2007.

Rohrer, F. and Berresheim, H.: Strong correlation between levels of tropospheric hydroxyl radicals and solar ultraviolet radiation, Nature,
565   442, 184–187, https://doi.org/10.1038/nature04924, 2006.

Rolph, G., Stein, A., and Stunder, B.: Real-time Environmental Applications and Display sYstem: READY, Environmental Modelling Software, 95, 210–228, https://doi.org/10.1016/j.envsoft.2017.06.025, 2017.

Sander, S. P., Friedl, R. R., Ravishankara, A. R., Kolb, C. E., Kurylo, M. J., Huie, R. E., Orkin, V. L., Molina, M. J., Moortgat, G. K., and Finlayson-Pitts, B. J.: Chemical Kinetics and Photochemical Data for Use in Atmospheric Studies Evaluation Number 14 NASA Panel
570   for Data Evaluation, http://jpldataeval.jpl.nasa.gov/, 2003.

Sarkar, C., Guenther, A. B., Park, J. H., Seco, R., Seco, R., Alves, E., Alves, E., Batalha, S., Santana, R., Kim, S., Smith, J., Tóta, J., and Vega, O.: PTR-TOF-MS eddy covariance measurements of isoprene and monoterpene fluxes from an eastern Amazonian rainforest, Atmospheric Chemistry and Physics, 20, 7179–7191, https://doi.org/10.5194/ACP-20-7179-2020, 2020.

Spracklen, D. V., Carslaw, K. S., Kulmala, M., Kerminen, V.-M., Mann, G. W., and Sihto, S. L.: The contribution of boundary layer
575   nucleation events to total particle concentrations on regional and global scales, Atmospheric Chemistry and Physics, 6, 5631–5648, https://doi.org/10.5194/ACP-6-5631-2006, 2006.

Spracklen, D. V., Carslaw, K. S., Kulmala, M., Kerminen, V. M., Sihto, S. L., Riipinen, I., Merikanto, J., Mann, G. W., Chipperfield, M. P., Wiedensohler, A., Birmili, W., and Lihavainen, H.: aContribution of particle formation to global cloud condensation nuclei concentrations, Geophysical Research Letters, 35, https://doi.org/10.1029/2007GL033038, 2008.

580   Spracklen, D. V., Carslaw, K. S., Merikanto, J., Mann, G. W., Reddington, C. L., Pickering, S., Ogren, J. A., Andrews, E., Baltensperger, U., Weingartner, E., Boy, M., Kulmala, M., Laakso, L., Lihavainen, H., Kivekäs, N., Komppula, M., Mihalopoulos, N., Kouvarakis, G., Jennings, S. G., O'Dowd, C., Birmili, W., Wiedensohler, A., Weller, R., Gras, J., Laj, P., Sellegri, K., Bonn, B., Krejci, R., Laaksonen, A., Hamed, A., Minikin, A., Harrison, R. M., Talbot, R., and Sun, J.: Explaining global surface aerosol number concentrations in terms of primary emissions and particle formation, Atmospheric Chemistry and Physics, 10, 4775–4793, https://doi.org/10.5194/ACP-10-4775-
585   2010, 2010.

Springston, S. R.: Sulfur Dioxide Monitor Instrument Handbook, DOE/SC-ARM-TR-180, 2016.

Springston, S. R.: Ozone Monitor (OZONE) Instrument Handbook, DOE/SC-ARM-TR-179, 2020.

Stein, A., Draxler, R., Rolph, G., Stunder, B., Cohen, M., and Ngan, F.: NOAA's HYSPLIT Atmospheric Transport and Dispersion Modeling System, Bulletin of the American Meteorological Society, 96, 2059–2077, https://doi.org/10.1175/BAMS-D-14-00110.1, 2015.

590   Stolzenburg, D., Simon, M., Ranjithkumar, A., Kürten, A., Lehtipalo, K., Lehtipalo, K., Gordon, H., Ehrhart, S., Finkenzeller, H., Pichelstorfer, L., Niemenen, T., He, X., Brilke, S., Xiao, M., Amorim, A., Baalbaki, R., Baccarini, A., Beck, L., Bräkling, S., Murillo, L., Chen, D., Chu, B., Dada, L., Dias, A., Dommen, J., Duplissy, J., El Haddad, I., Fischer, L., Carracedo, L., Heinritzi, M., Kim, C., Koenig, T., Kong,

W., Lamkaddam, H., Lee, C., Leiminger, M., Li, Z., Makhmutov, V., Manninen, H., Marie, G., Marten, R., Müller, T., Nie, W., Partoll, E., Petäjä, T., Pfeifer, J., Philippov, M., Rissanen, M., Rörup, B., Schobesberger, S., Schuchmann, S., Shen, J., Sipilä, M., Steiner, G., Stozhkov, Y., Tauber, C., Tham., Y., Tomé, A., Vazquez-Pufleau, M., Wagner, A., Wang, M., Wang, Y., Weber, S., Wimmer, D., Wlasits, P., Wu, Y., Ye, Q., Zauner-Wieczorek, M., Baltensperger, U., Carslaw, K., Curtius, J., Donahue, N., Flagan, R., Hansel, A., Kulmala, M., Lelieveld, J., Volkamer, R., Kirkby, J., and Winkler, P.: Enhanced growth rate of atmospheric particles from sulfuric acid, Atmospheric Chemistry and Physics, 20, 7359–7372, https://doi.org/10.5194/acp-20-7359-2020, 2020.

Stolzenburg, M. R., McMurry, P. H., Sakurai, H., Smith, J. N., Mauldin, R. L., Eisele, F. L., and Clement, C. F.: Growth rates of freshly nucle-ated atmospheric particles in Atlanta, Journal of Geophysical Research Atmospheres, 110, 1–10, https://doi.org/10.1029/2005JD005935, 2005.

Tanner, D. J., Jefferson, A., and Eisele, F. L.: Selected ion chemical ionization mass spectrometric measurement of OH, Journal of Geophys-ical Research Atmospheres, 102, 6415–6425, https://doi.org/10.1029/96jd03919, 1997.

Weber, R. J., Marti, J. J., McMurry, P. H., Eisele, F. L., Tanner, D. J., and Jefferson, A.: Measured atmospheric new particle formation rates: Implications for nucleation mechanisms, Chemical Engineering Communications, 151, 53–64, https://doi.org/10.1080/00986449608936541, 1996.

Weber, R. J., Marti, J. J., McMurry, P. H., Eisele, F. L., Tanner, D. J., and Jefferson, A.: Measurements of new particle forma-tion and ultrafine particle growth rates at a clean continental site, Journal of Geophysical Research Atmospheres, 102, 4375–4385, https://doi.org/10.1029/96jd03656, 1997.

Wehner, B., Petäjä, T., Boy, M., Engler, C., Birmili, W., Tuch, T., Wiedensohler, A., and Kulmala, M.: The contribution of sulfu-ric acid and non-volatile compounds on the growth of freshly formed atmospheric aerosols, Geophysical Research Letters, 32, 1–4, https://doi.org/10.1029/2005GL023827, 2005.

Yamasoe, A., Artaxo, P., Miguel, A. H., and Allen, A. G.: Chemical composition of aerosol particles from direct emissions of vegetation "res in the Amazon Basin: water-soluble species and trace elements, Atmospheric Environment, 34, 1641–1653, 2000.

Yao, L., Garmash, O., Bianchi, F., Zheng, J., Yan, C., Kontkanen, J., Junninen, H., Mazon, S. B., Ehn, M., Paasonen, P., Sipilä, M., Wang, M., Wang, X., Xiao, S., Chen, H., Lu, Y., Zhang, B., Wang, D., Fu, Q., Geng, F., Li, L., Wang, H., Qiao, L., Yang, X., Chen, J., Kerminen, V.-M., Petäjä, T., Worsnop, D., Kulmala, M., and Wang, L.: Atmospheric new particle formation from sulfuric acid and amines in a Chinese megacity, Science, 361, 278–281, https://doi.org/10.1126/science.aao4839, 2018.